

Application of low transformation-temperature filler to reduce the residual stresses in welded component

K. Azizpour¹, H. moshayedi^{2*}, I. Sattari-far¹

¹ Mechanical Engineering Department, Amirkabir University of Technology, Tehran, Iran.

² Young Researchers and Elite Club, Buinzahra Branch, Islamic Azad University, Buinzahra, Iran.

Phone: +98 21 64543498

*Email: h_moshayedi@yahoo.com

ABSTRACT

Tensile residual stress is a major issue in integrity of the welded structures. Undesirable tensile residual stress in welding may reduce fracture toughness and fatigue life of welded structures. The low transformation-temperature (LTT) fillers, due to introducing compressive residual stresses caused by prior martensitic transformation, can reduce tensile residual stresses in the weld zone. The effects of using LTT fillers on welding residual stresses of high strength steel sheets are studied and compared with conventional fillers. 3D finite element simulations including coupled thermal-metallurgical-mechanical analyses are developed using SYSWELD software to predict the welding residual stresses. For validation of the finite element model, the residual stresses are measured through hole drilling strain gage method. The results indicate that using the LTT fillers cause a decrease of the longitudinal tensile residual stresses of the weld metal from 554 MPa to 216 MPa in comparison with conventional fillers. The transverse residual stresses of the weld line are changed from tensile 156 MPa to compressive 289 MPa with using LTT fillers instead of conventional fillers.

Keywords: Welding residual stress; low transformation-temperature filler; finite element simulation; coupled thermal-metallurgical-mechanical analyses; phase transformation.

INTRODUCTION

Fusion welding provides a very economical method for joining the structures and is considered an essential process in the industry [1]. Due to high local temperature changes in the welding area, plastic deformations and consequently tensile residual stresses would have occurred. These stresses reduce the structural strength significantly and can affect the behavior of the structure, especially in fatigue, failure and corrosion conditions [2].

According to the applications of welding in the industries and the need for a desirable safety factor of the welded components, many attempts have been performed in order to reduce the tensile residual stresses [3]. Structures with lower tensile residual stresses show better properties including fatigue life, resistance to stress corrosion and sensitivity to hot

and cold cracks. Several methods such as post weld heat or mechanical treatments, reduce tensile residual stresses by the creation of compressive residual stress after welding. However, these methods are often expensive and time-consuming. It is desired to control residual stresses during the welding process. In the recent decade, the concept of creating compressive residual stress is by controlling phase transformation during welding has been proposed counteracting the tensile residual stress and improve the mechanical behavior of welded structures [4].

Using low transformation temperature fillers, the resulted expansion would counteract the thermal contraction caused by cooling of the weld, which would consequently reduce the tensile residual stress and distortion. Compared to the conventional fillers, these materials can decrease the start temperature of martensite transformation (M_s). Therefore, due to the martensite transformation at low temperature, the tensile residual stresses would be decreased or even transformed to the compressive residual stress [5].

Recently, by means of empirical formulas that developed to predict the martensite start temperature, welding fillers have been designed with different combinations and different martensite start temperatures [5]. Knowing the residual stresses level would lead to the more accurate design of engineering structures. However, the measurement of the residual stresses by experimental methods are often expensive and time-consuming. A finite element method is a useful tool for investigating the thermo-mechanical behavior of the welded structures that have been developed in recent decades for predicting welding residual stresses. In most of the conducted simulations of welding metallurgical changes have been ignored, due to the complexity of the Thermo-Mechanical-Metallurgical analysis. While in high carbon steels, alloy steels and high strength steels, this assumption can lead to significant errors in predicting the welding residual stresses.

Some of the researches have been conducted on the applications of martensite transformation and LTT filler in reducing tensile residual stresses, producing compressive residual stresses and improving the fatigue life of the welded joints.

Kannengiesser et al [6], investigated the effects of LTT filler with 8, 10 and 12 percentages of nickel in high strength steel S690 on the residual stresses and martensite transformation. Their results in two modes of martensite and austenite showed that the compressive residual stress would be formed in the FZ and HAZ as a result of martensite transformation. Distribution of the residual stresses in the martensite phase for different percent of nickel is similar. However, the amount of residual stresses in center of the welding line is different and decreases with an increase in the nickel percentage.

Camilleri et al [7], studied the ability of LTT fillers in reducing the residual stresses and unwanted distortions. Their investigations were conducted on the welded plates of DH36 steel using 3 type filler, which one of them was LTT filler consisted of 11 percent nickel and no chromium. Insignificant differences were observed between the distortion of the welds with common filler and LTT filler, while the residual stresses were very different and LTT filler had even form compressive residual stresses. Controlling the distortion value and physical properties of high strength steels welded with LTT filler were studied by Ozdemir et al [8]. Comparisons showed the less distortion in welding with LTT filler compared to conventional filler, and the lower M_s temperature would lead to less distortion. Results of hardness measurement and the tensile test showed higher hardness and higher tensile strength in welding with LTT filler, and also less percentage of retained austenite in martensite would lead to a higher weld hardness.

Ozdemir et al [9], examined the influence of welding with LTT filler on microstructure and mechanical properties of high strength steel Weldox 700. They compared the welded joints in terms of microstructure, hardness, bending, tensile and impact tests. According to their results, the microstructure of welding with LTT filler is martensitic, so they gain higher hardness than base metal in the welding line. Also, yield strength and tensile strength of the LTT joint is higher compared to the conventional joint, however, the percentage of elongation, bending strength and fracture energy in the conventional joint is higher.

Barsoum and Gvstafsson [10], investigated the effect of LTT filler on the residual stresses and fatigue in high strength steels welding and observed that LTT joints have better resistance compared to the conventional joints at constant amplitude fatigue test (CA), while variable amplitude fatigue test (VA) showed different results and in high stresses, LTT and conventional overlap as a result of relaxing compressive residual stresses.

The effect of dilution and strength of the base metal on the residual stresses distribution in multi-pass welding using LTT fillers has been studied by Ramjavn et al [11]. They concluded that excessive lowering of M_s is not effective in reducing the tensile residual stress and creation of compressive residual stress, in addition, the residual stresses rise again for too low M_s . Also, for a greater degree of dilution and greater amounts of base metal in the fusion zone (FZ), the effect of LTT filler becomes less.

Moat and et al [12], investigated the effect of using LTT fillers on multipass welds residual stress. They showed that the stress mitigating the effect of LTT alloy is indeed diminished during multi pass welding. They proposed a carefully selected elevated interpass hold temperature and demonstrated that this restores the LTT capability to successfully mitigate residual tensile stresses. Application of LTT filler in MAG welding under structural restraint has been studied by Vollert et al [13]. Their study was conducted a strong effect on the local strain evolution and the formation of compressive strain. Their results indicate that the restraint volume expansion during the postponed austenite to martensite transformation of the LTT weld filler, counteracts the thermal shrinkage. Gach et al [14], studied the residual stress reduction of laser beam welds by use of LTT filler materials in carbon manganese steels. Different welding parameters were investigated in different dilution levels for the LTT filler material. Results of displacements measurement after welding showed that LTT wires can be used to mitigate distortion during laser beam welding.

As a new method, the effect of using LTT fillers on the formation of residual stresses in welding has been investigated by Deng and Jiang [15]. They concluded that that the low temperature phase transformation has a significant effect on the evolution of residual stress; the LTT 'smart' alloy utilizes this effect to mitigate the tensile residual stress. They reported that the application of LTT alloy effectively improves the state of residual stress in high strength alloy steel. Since the welding process is widely used in hi-tech industries such as aerospace, nuclear and refinery, reducing the tensile residual stresses is very important, technically and economically. According to the importance of martensitic transformation in the formation of residual stresses in welding with LTT filler, developing a finite element model considering the phase changes can be useful.

In this study, the effect of LTT fillers on the welding residual stresses is investigated. Two sheets of high-strength steel are welded by LTT filler and a conventional filler, the residual stresses are measured. In order to predict the residual stress, a Three-dimensional finite element model is developed in SYSWELD and the results are compared with the

experimental data. Finally, the effect of using LTT filler is discussed according to the comparison results.

MECHANISM OF LTT FILLERS EFFECTS

Martensite transformation in LTT fillers

Martensite is formed by rapid cooling and diffusionless transformation of austenite in steel and constitutes a metastable BCT (body-centered tetragonal) phase. Martensite has exactly the same chemical composition of the base austenite [16]. Austenite decomposition begins when the temperature drops to martensite start point and due to the quick phase transformation, nucleation and grain growth would not be possible [17].

Martensite transformation process is defined by two different temperatures, M_s or martensite start, at which austenite transformation into martensite begins, and M_f or martensite finish, at which 100% of martensite is formed [18].

Alloy chemical composition and the cooling rate after welding affect M_s and M_f , significantly. By cooling, contraction of FZ is occurred, which would lead to the creation of tensile residual stresses. According to the lower density of martensite compared to austenite, martensite formation leads to expansion. Since the cooling rate of the weld region is higher, more amount of martensite would form there which cause more expansion in this region. The expansion induced by phase transformation compromises thermal contraction. According to the fact that pure compressive residual stresses are created once expansion surpasses thermal contraction; hence, it is better that martensite transformation starts at a temperature as low as possible so that the completion temperature (M_f) is still above the point upon which the weld is allowed to cool [19].

Figure 1 shows the differences in variations of stress and strain during cooling in LTT and normal fillers. As it can be seen in Figure 1(a), cooling-induced contraction is the dominant factor in the normal filler, and expansion occurs from 600°C to 500°C in austenite decomposition process. After transformation, the weld is contracted again and tensile residual stresses are formed at room temperature. In LTT filler, the dominant factor is the expansion induced by austenite to martensite transformation at 200°C, which continues up to room temperature. Expansion at low temperatures leads to a reduction in tensile residual stresses and also creation of compressive residual stresses in the FZ and its adjacent areas [20] (Figure 1(b)).

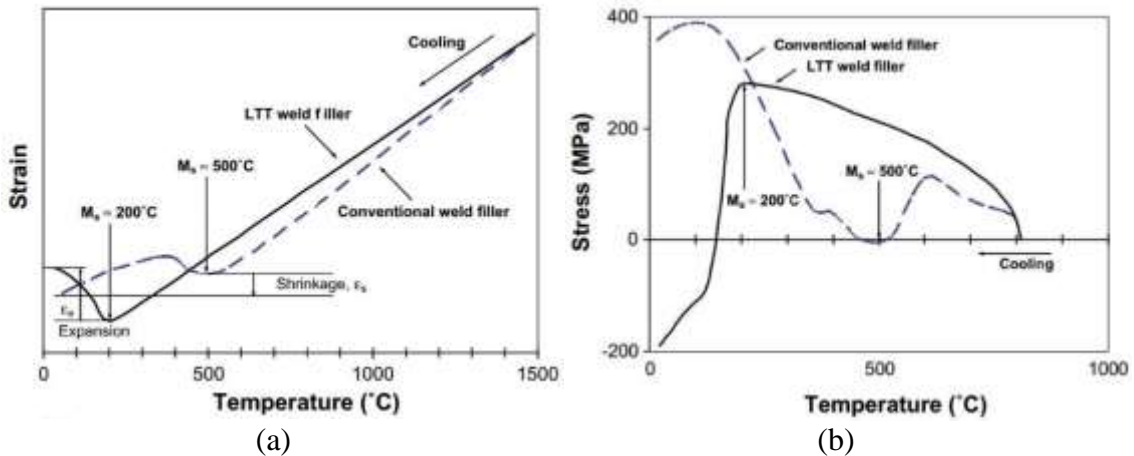


Figure 1. Strain and stress variations during cooling: a) strain, b) stress [20].

Martensite transformation cannot be completed when the martensite finish temperature is lower than room temperature and consequently less martensite may be formed. On the other hand, residual stresses are directly related to the martensite quantity; thus, it may be stated that martensite transformation temperatures are the most important factors in development of compressive residual stresses using LTT fillers [19].

CHEMICAL COMPOSITION

In addition to facilitation of achieving M_s at low temperature (in order to obtain a maximum decrease in tensile residual stresses), elements which are used in manufacturing LTT fillers have to satisfy design requirements. The strength of LTT alloys should be higher or equal to that of the base metal and also be sufficiently tough. In addition, sensitivity to hot and cold cracks as well as corrosion resistance should be considered in designing LTT fillers. The main difference in the chemical composition of normal and LTT fillers is the presence of high contents of Ni and Cr (up to 10 percent) in the latter one, which is low in the normal fillers [21]. In the following, the effects of adding Ni and Cr on steel is discussed.

Nickel reduces the eutectoid temperature. In fact, eutectoid temperature is gradually reduced during cooling by increasing the nickel percentage (approximately 10°C for each percent). In cooling, however, this reduction is irregular and more noticeable. The result of increasing the nickel amount is similar to increasing the carbon steel cooling rate. It hinders the formation of pearlite and leads to the creation of a martensitic structure after heat treatment. The required amount of nickel depends on the cooling rate and thickness of cast parts [22].

Chromium is soluble in iron in both alpha and gamma phases. However, in the presence of carbon, formation of carbides (such as Cr_3C) is possible once the chromium content reaches 15 percent. Other possible carbides are Cr_4C , Cr_7C_3 and Cr_3C_2 . Stainless steels usually contain Cr_4C . Chromium pearlite steels containing 2% Cr are extremely sensitive to cooling rate and temperature before quenching. By with increasing the Cr content, Eutectic point shifts towards the left; thus, austenite area becomes smaller.

Accordingly, carbon solubility in austenite is reduced too. In addition, T.T.T diagram is shifted towards the right and M_s line is moved downward [22].

Nickel and Chromium: Ni-bearing steels are very useful due to the high strength, ductility and toughness; whereas, Cr-bearing steels are of considerable interest due to hardness and wear resistance. Combination of nickel and chromium leads to the production of steel with all of these properties (sometimes intensified), without any disadvantages. Low Ni-Cr steels with low amount of carbon are used for hardening; while, adding a considerable amount of nickel and chromium would result in an improved and high-temperature oxidation resistance [22].

Most of the designed LTT fillers in the last two decades contained combinations of Ni and Cr as well as low amounts of carbon. The recommended range for nickel content is from 5% to 11% in order to reduce M_s temperature and also improve toughness. Chromium content, should be within the same range for M_s reduction, unless corrosion resistance is required, in that case, 12% or more chromium is added to achieve stainless steel. Low carbon content is recommended to avoid formation of chromium carbides.

MATERIALS AND EXPERIMENTAL PROCEDURE

Experiments were aimed to investigate the effects of LTT fillers on the residual stresses and also, verification of the developed finite element model. In this study, high-strength Domex 700 MC steel sheets were butt welded using normal and LTT fillers. Domex steel was rolled thermo-mechanically in a modern apparatus in which heating, rolling and cooling processes were precisely controlled. High-strength steels are used for reducing weight or increasing load capacity. ER410NiMo stainless martensitic alloy was used as the LTT filler. It should be noted that among commercial fillers, ER410 NiMo which is in martensitic stainless steel fillers category, has the best composition to achieve optimum M_s temperature with the chemical composition given in Table 2. In addition, ER70S-6, a widely used carbon steel filler was used as the normal filler. Chemical compositions of these fillers and the base metal are given in Tables 1-3.

Table 1. The chemical composition of Domex 700 MC steel.

C	Mn	Si	P	S	Al	Nb	V	Ti
max	max	max	max	max	max	max	max	max
0.12	2.10	0.10	0.025	0.010	0.015	0.09	0.20	0.15

Table 2. The chemical composition of ER410 NiMo.

C	Mn	Si	P	S	Cr	Ni	Mo	Cu
0.03	0.8	0.25	0.01	0.01	12	4.5	0.6	0.05

Table 3. The chemical composition of ER70S-6.

C	Si	Ni	Mo	Cu	S
0.06-0.15	0.8-1.15	0.15 max	0.15 max	0.50 max	0.035 max
Cr	Fe	Mn	P	V	other
0.15 max	residual	1.4-1.85	0.025 max	0.03 max	0.50 max

M_s values of fillers and the base metal were calculated according to Liu and Alghamdi [23] results, using the Equation (1) proposed by Self and Olsena:

$$M_s (\text{°C}) = 521 - 14.3Cr - 17.5Ni - 28.9Mn - 37.6Si - 350C - 29.5Mo + 23.1(Cr + Mo) - 1.19Cr_x Ni \quad (1)$$

Calculated temperatures are given in Table 4. It may be observed that M_s of LTT was quite less than those of the normal filler and the base metal.

Table 4. Calculated M_s temperatures for materials.

Self & Olson	Domex 700 MC	ER70S-6	ER410 NiMo
M_s (°C)	445	400	166

Preparation and welding of samples

Samples were cut from a large sheet. All the surfaces were cleaned and edges were prepared by beveling, prior to welding. Samples geometry, joint type and root distance are illustrated in Figure 2.

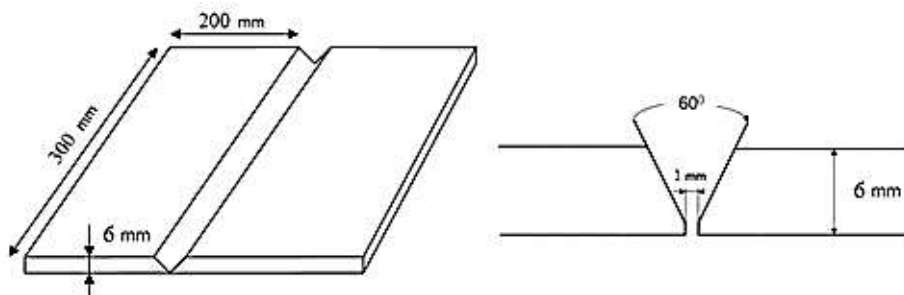


Figure 2. The geometry of samples.

Four-passes GTAW process with consumable filler was applied. Welding parameters are provided in Table 5.

Table 5. Welding parameters.

Process	Filler diameter (mm)	Current type	Current (A)	Voltage (V)	Speed (mm/s)	Inert gas flow rate (mm/s)
GTAW	2.4	DC	130	20	3	15
GTAW	2.4	DC	140	20	3	15
GTAW	2.4	DC	150	20	3	15
GTAW	2.4	DC	160	20	3	15

Samples were welded along with rolling direction and no heat treatment was performed on samples prior and after welding. Clamp and bracket mechanisms were employed for fixing the sheets during the welding process (Figure 3). Final welded samples (prior to residual stress measurement tests) are shown in Figure 4.

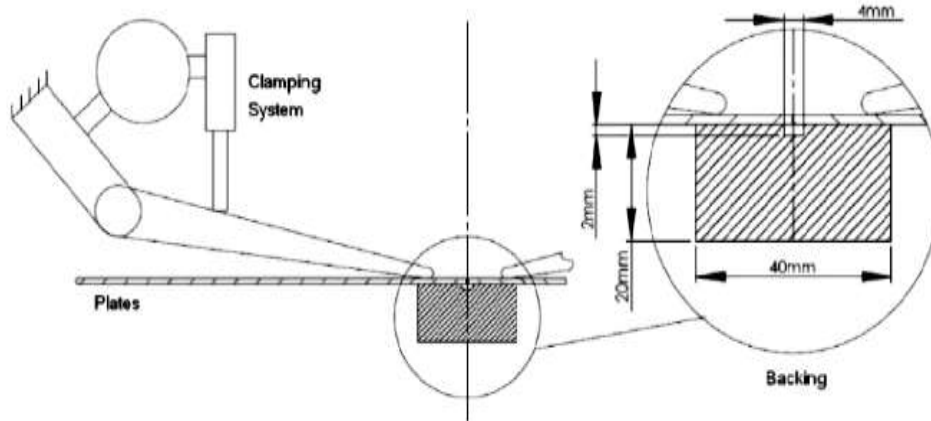


Figure 3. Specimens clamping set-up during welding.

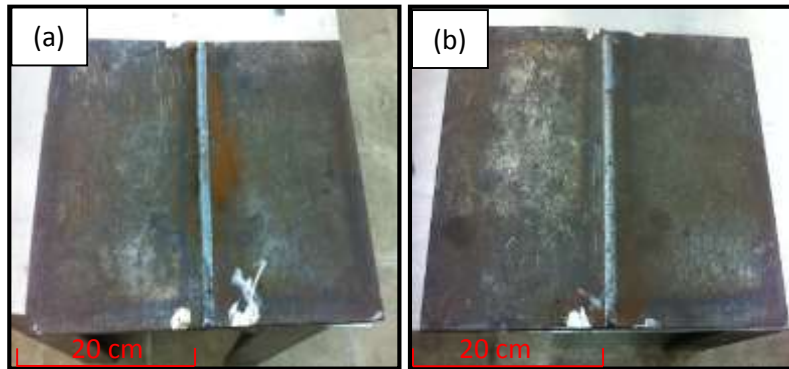


Figure 4. Welded samples: (a) welded by ER70S-6, (b) welded by ER410-NiMo.

Residual stress measurement

Residual stresses were measured by means of the hole-drilling strain-gage method. Technical details and calculation procedure can be found in ASTM E837-13 [24]. As indicated in Figure 5, the strain gages were located in the middle section of the sheet and perpendicular to the weld direction. The test set up is shown in Figure 6. Measured results are presented in Tables 6 and 7, respectively.

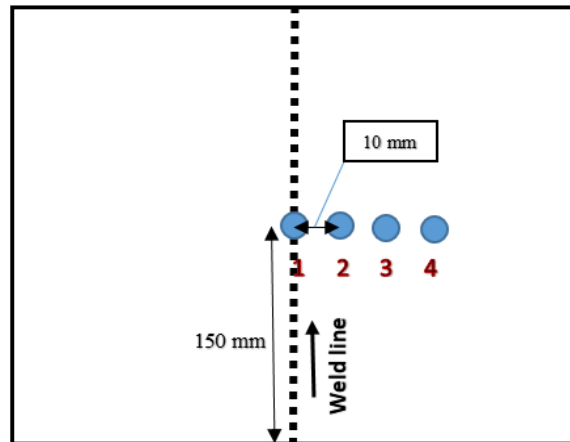


Figure 5. Location of strain gages installed on each sample.

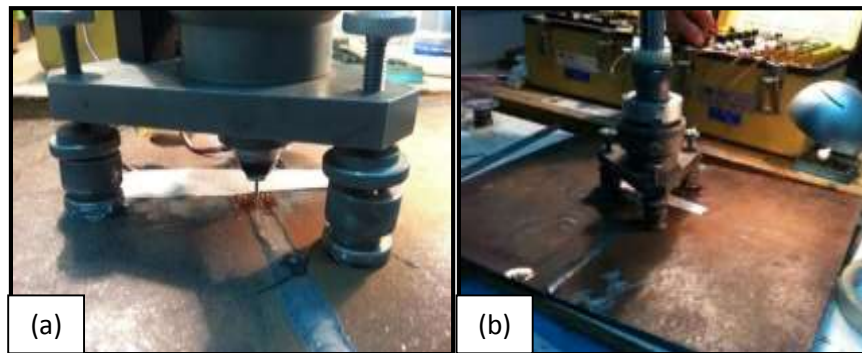


Figure 6. Hole-drilling strain-gage test: (a) set up, (b) drilling.

Table 6. Results of residual stress measurement in ER70S-6.

Distance from the weld center	Longitudinal residual stress (MPa)	Transverse residual stress (MPa)
0	554	156
15	272	16
30	-65	-20
45	-145	-22

Table 7. Results of residual stress measurement in ER410-NiMo.

Distance from the weld center	Longitudinal residual stress (MPa)	Transverse residual stress (MPa)
0	216	-289
15	254	65
30	-76	40
45	-183	10

FINITE ELEMENT MODELING

Two 3-D models were developed to simulate butt welding of samples in SYSWELD software. Analyses were carried out in form of fully coupled thermo-metallurgical and unilateral mechanical-metallurgical-thermal coupled. Thermal analyses are first performed and temperature and phase percentages are obtained. Afterwards, an uncoupled mechanical analysis is performed based on the thermal-metallurgical history. Mechanical results are dependent on both temperature and metallurgical histories. Considering the metallurgical transformations in the calculations is important due to two aspects: first, thermo-mechanical properties vary with respect to phases; second, plastic deformation phenomenon may significantly affect residual stresses. General structure of simulation in SYSWELD is shown in Figure 7.

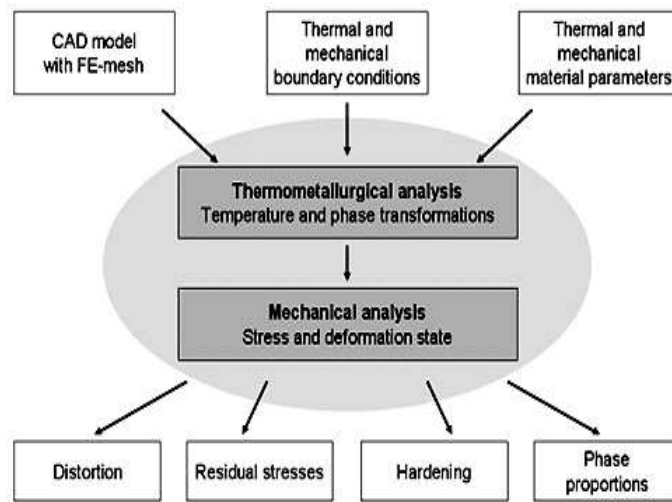


Figure 7. Structure of welding simulation in SYSWELD.

The models were developed similar to the experimental samples. Mesh sensitivity was performed and optional mesh configuration was selected. There were 24000 elements in each model. Figure 8 illustrates the geometry and mesh configuration of the models.

Welding process was simulated based on welding parameters in Table 5. Filler materials were modelled by element birth and death technique. The temperature-dependent values of thermal conductivity and specific heat capacity are summarized in Table 8. Density was assumed to be 7820 kg.m^{-3} at room temperature and 7490 kg.m^{-3} at 1400°C . The Poisson's ratio was assumed to be 0.29 for the LTT filler and 0.26 for the base metal and normal filler, independent of temperature. thermal expansion coefficient was assumed to $9.2\text{E-}6 \text{ 1/}^\circ\text{C}$ for the LTT filler and $8.5\text{E-}6 \text{ 1/}^\circ\text{C}$ for the base metal and normal filler, independent of temperature [25].



Figure 8. Mesh configuration of the models.

Applied temperature-dependent mechanical properties are listed in Table 9. The yield and ultimate stresses at room temperature were taken from experimental tensile tests. For higher temperatures, reported properties in literatures were used and scaled based on room temperature values [25].

Table 8. Thermo-physical material properties for welding simulation [25].

Temperature (°C)	Specific heat (J/(kg.°C))				Conductivity (W/(m.°C))			
	Base metal	Normal filler	LTT filler		Base metal	Normal filler	LTT filler	
			Austenite Phase	Martensite Phase			Austenite Phase	Martensite Phase
20	510	452	632	460	33.9	17.5	16.0	16.0
100	519	473	633	485	-	18.1	-	-
200	532	498	635	524	34.6	19.4	18.7	18.7
300	548	512	639	548	-	21.5	-	-
400	579	526	645	615	36.1	22.2	21.3	21.3
500	669	536	668	680	-	23.1	-	-
600	751	543	691	748	35.3	24.6	22.2	22.2
700	1141	547	702	973	-	25.4	-	-
800	815	557	730	1418	31.9	26.3	24.5	24.5
900	699	564	679	1179	-	27.5	-	-
1000	579	575	648	981	27.7	28.4	28.7	28.7
1100	587	586	651	897	-	29.6	-	-
1200	601	599	656	801	24.6	30.7	29.9	29.9
1300	614	614	659	744	-	31.5	-	-
1400	626	625	662	698	22.4	32.3	32.2	32.2
1500	673	631	664	655	33.1	33.9	33.03	33.03

Table 9. Yield strength dependency on temperature for the weld and base metals for the welding simulation [25].

Temperature (°C)	Yield stress (MPa)				Elasticity modulus (GPa)			
	Base metal	Normal filler	LTT filler		Base metal	Normal filler	LTT filler	
			Austenite Phase	Martensite Phase			Austenite Phase	Martensite Phase
20	800	440	240	1100	210	218	218	215
100	789	412	226	1076	205	211	211	208
200	772	384	207	1017	200	205	205	200
300	701	343	191	978	191	193	193	195
400	653	266	164	924	175	186	186	186
500	579	209	129	826	159	177	177	174
600	454	169	103	645	135	161	161	162
700	321	134	78	332	103	153	153	142
800	120	107	66	112	78	118	118	119
900	72	77	51	58	57	39	39	72
1000	42	51	35	44	35	18	18	30
1100	21	45	26	24	22	12	12	16
1200	10	31	15	11	11	9.8	9.8	8
1300	7	16	7	5	7	6	6	5
1400	5	9	3	3	3	3	3	3
1500	1	5	1	2	1	1	1	1

Goldak’s double ellipsoid 3-D model was used for simulating the heat source [26], which is schematically illustrated in Figure 9. In this model, two different ellipsoid halves are considered for creation of heat source with different equations. Heat flux equations in front and back ellipsoids of the welding arc are as Equations (2-3):

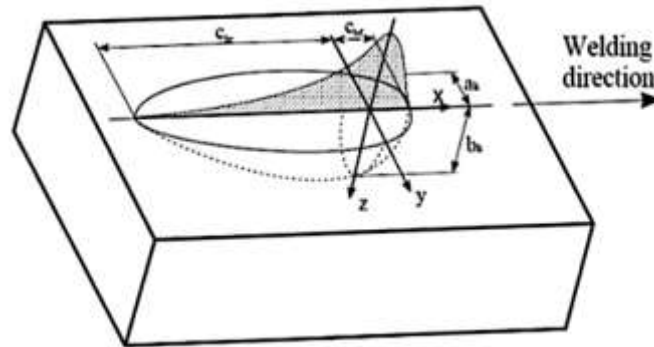


Figure 9. Goldak’s ellipsoid heat source

$$Q(x, y, z) = \frac{6\sqrt{3}r_f Q}{a_h b_h c_{hf} \pi \sqrt{\pi}} \exp\left(-\frac{3x^2}{c_{hf}^2} - \frac{3y^2}{a_h^2} - \frac{3z^2}{b_h^2}\right) \quad (2)$$

$$Q(x, y, z) = \frac{6\sqrt{3}r_b Q}{a_h b_h c_{hb} \pi \sqrt{\pi}} \exp\left(-\frac{3x^2}{c_{hb}^2} - \frac{3y^2}{a_h^2} - \frac{3z^2}{b_h^2}\right) \quad (3)$$

Where a_h , b_h , c_{hf} and c_{hb} are the parameters of double ellipsoid heat source as shown in Figure 9. r_f and r_b are the thermal proportion coefficients at front and back arc regions. Values of r_f and r_b are defined through Equations (4-6):

$$r_f = 2c_{hf} / (c_{hf} + c_{hb}) \quad (4)$$

$$r_b = 2c_{hb} / (c_{hf} + c_{hb}) \quad (5)$$

$$r_f + r_b = 2 \quad (6)$$

Heat input, Q , can be calculated from Equation (7).

$$Q = \eta V I \quad (7)$$

Where, I is the current, V is the voltage and η is the welding arc efficiency, which is considered to be 60% for TIG welding technique [27]. Goldak's model parameters used here are given in Table 10. The dimensions of the molten material pond proposed method by [28] were employed. After each pass, 100 s cooling time was allocated prior to start of the next pass, to reach allowable inter-pass temperature.

Table 10. Parameters of volumetric Goldak's double ellipsoid model.

Parameter	Value (mm)
c_{hf}	12
c_{hb}	16
a_h	10
b_h	2
r_f	1.5
r_b	0.5

Thermal calculations were performed based on the repeated solution of the modified thermal equation considering latent heat of solidification/fusion as well as phase transformation heat in solid state. The equation is written as Equation (8) [29]:

$$\rho C \frac{\partial \theta}{\partial t} = \nabla(\lambda \nabla \theta) - \sum_{i \in j} L_{ij} \cdot A_{ij} \quad (8)$$

Where L_{ij} is latent heat in the transformation of phase i into phase j , A_{ij} is the percentage of phase i transformed to phase j in the time unit, C is specific heat and λ is conductivity with respect to the percentage of different phases calculated by the Equations (9-10):

$$C = \sum_i P_i C_i \tag{9}$$

$$\lambda = \sum_i P_i \lambda_i \tag{10}$$

Special heats of phases C_i and phase transformation heat are calculated in Equations (11-12) as functions of phase enthalpy, H_i [29]:

$$C_i = \frac{dH_i}{d\theta} \tag{11}$$

$$L_{ij} = H_j - H_i \tag{12}$$

Thermal boundary conditions were considered as convection and radiation. Convection boundary conditions were applied at all surfaces. Initial temperature of the model was considered at 25°C. Convection was modelled using the Equation (13):

$$\{q\}^T \{\eta\} = h_f (T_s - T_b) \tag{13}$$

Where $h_f = 25 \text{ W/m}^2\text{K}$ is convection coefficient, T_b is room temperature and T_s is surface temperature [30]. Radiation was modelled through Equation (14):

$$Q_i = \sigma_{bol} \varepsilon_i F_{ij} A_i (T_i^4 - T_j^4) \tag{14}$$

Where $\sigma_{bol} = 5.67 \times 10^{-8} \text{ W/m}^2\text{K}^4$ is Stephen-Boltzmann constant, $\varepsilon = 0.8$ is effective emissivity coefficient and F is shape factor. Main equations of mechanical analysis include equilibrium and base equations defined through Equations (15-16) [30]:

$$\sigma_{ij} + \rho b_i = 0 \tag{15}$$

$$\sigma_{ij} = \sigma_{ji} \tag{16}$$

Where σ_{ij} is stress tensor and b_i is body force. The second equation implies symmetry of the stress tensor. In the base equations for the model of thermelasto-plastic materials, the model is considered using von Mises yield criterion and isotropic strain hardening rule which can be written as Equations (17-18) [30]:

$$[d\sigma] = [D^{\varepsilon P}] [d\varepsilon] - [C^{th}] dT \tag{17}$$

$$[D^{\varepsilon P}] = [D^{\varepsilon}] + [D^P] \tag{18}$$

Where $[D^e]$ is elastic hardness matrix, $[D^p]$ is plastic hardness matrix, $[C^{th}]$ is thermal hardness matrix, $d\sigma$ is stress component, $d\varepsilon$ is strain component and dT is temperature component.

Nodes on two sides of the weld line were constrained in direction of normal to the sheet surface in order to simulate mechanical constraining conditions of welding. The constraint was deactivated after welding. Two nodes were constrained at one of its corners in three directions in order to maintain static balance of model. The mechanical boundary conditions are shown in Figure 10.

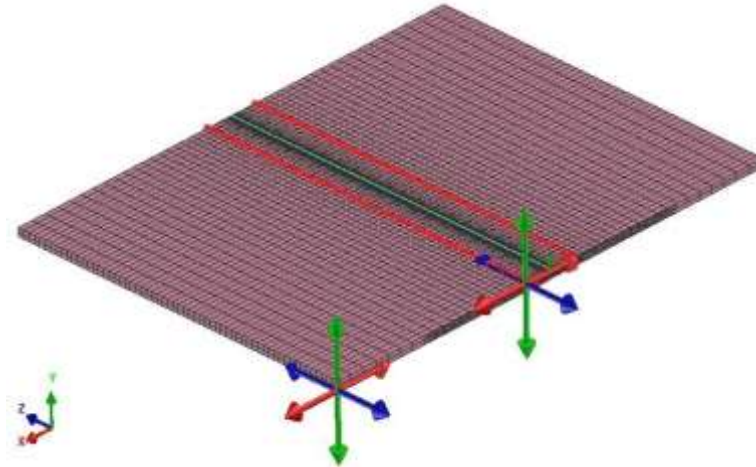


Figure 10. Mechanical boundary layers of models.

RESULTS AND DISCUSSION

Verification of finite element models

In order to verify the finite element models, the residual stresses results obtained from the reference models were compared with the experiments. Comparisons of longitudinal and transverse residual stresses are illustrated in Figs. 11 and 12, respectively.

It can be concluded that predicted longitudinal and transverse residual stresses are in a good agreement with the experimental results. Hence, other models with similar geometry and different conditions could be successfully simulated.

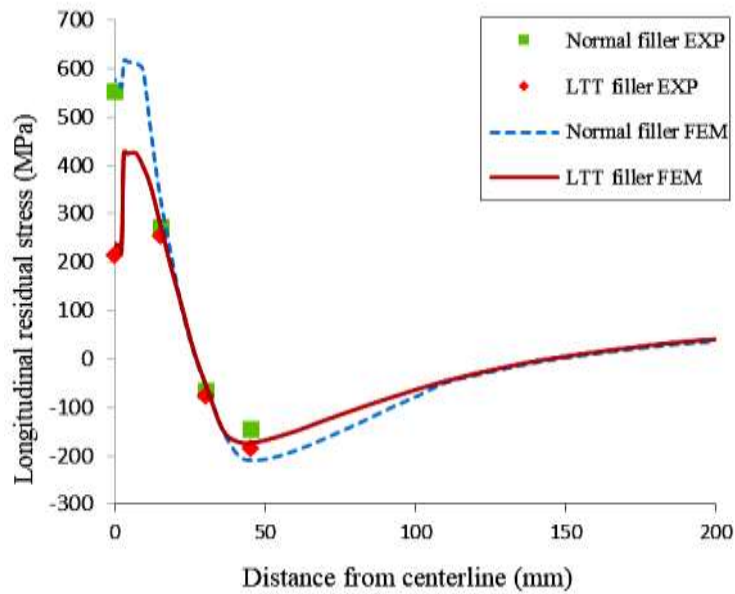


Figure 11. Predicted and measured longitudinal residual stresses for LTT and normal fillers.

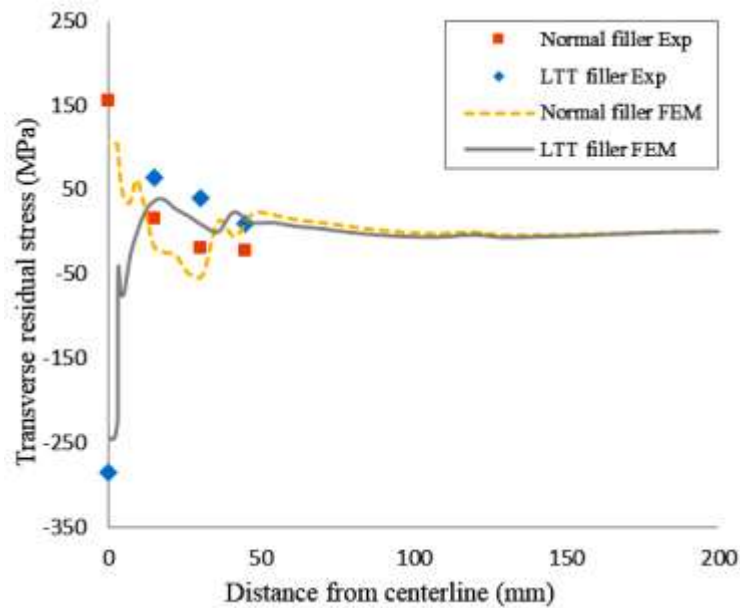


Figure 12. Predicted and measured transverse residual stresses for LTT and normal fillers.

Generally, in the butt welding process of a plate, the presence of high local heat flux from the heat source causes an intense temperature gradient in the piece, which leads to non-uniform thermal strains in the weld and surrounding areas. These thermal strains lead to the formation of welding residual stresses. During shrinkage resulted from cooling down of the weld zone, surrounding areas which do not experience high temperature, tend to prevent the

shrinkage of weld zone which encounters as inherent constraints. Therefore, tensile residual stresses are usually generated in the weld zone. Any volume changing process during cooling down of weld zone may change residual stress forming procedure and hence affect residual stress distribution. Therefore, volume changes due to metallurgical phase transformation during cooling could play a key role in changing the amount of residual stresses in weld zone. The idea of using LTT fillers is to achieve maximum possible expansion due to phase transformation at a low temperature in which thermal strain changes are insignificant and thus the expansion due to phase transformation could not be compensated by thermal shrinkage.

As it is clear from the experiment results, the longitudinal stress in the weld line center of the sample welded via normal filler was 554 MPa, which is decreased by 61% and decrease to 216 MPa using LTT filler. Stress values at the second point were 272 MPa and 254 MPa, for normal and LTT filler, respectively (decreased by 7%). In the austenitic-martensite phase transformation due to the relative difference in cell size between the BCC martensite structure and the FCC austenite structure, 4.3 percent increase in volume is generated. This increase in volume is in counteracting with thermal contraction. On the other hand, since martensitic phase transformation occurs at a relatively low temperature which formation and changes of thermal strains are not sensible, expansion due to phase transformation could not be compensated with thermal strains, and as a result tensile residual stresses have greatly decreased. So that the longitudinal residual stress in the weld center was changed from 554 MPa for conventional welding to 216 MPa for LTT filler weld and transverse residual stress from 156 MPa to 289 MPa compression. Using the LTT filler leads to formation of martensite in the weld zone; which is more concentrated in the center and fades at distant areas. Transverse residual stresses in weld line center for samples welded with normal and LTT fillers were 156 MPa and -289 MPa, respectively. The effect of LTT filler on the longitudinal and transverse residual stresses is very clear. Transverse residual stresses at distance of 15 mm of the weld line were 16 MPa for normal filler and 65 MPa for LTT filler; the increase is due to self-equilibrium of residual stresses.

Distribution of the longitudinal residual stresses in welding with conventional and LTT fillers at the middle of samples are compared in Figure 13. It can be observed that conventional filler welding leads to creation of tensile stresses in weld zone and its adjacent areas, which is equal to 576 MPa in the weld center with the maximum value occurring in HAZ and weld boundary. Maximum longitudinal residual stress is 619 MPa (77% of yield stress). Stresses begin to decrease rapidly at a distance of 7 mm from the weld center and reach to zero at 28 mm.

In welding with LTT filler, the longitudinal residual stresses in the weld zone are between 278 and 300 MPa at distance of 2mm from the weld center. Then they increase up to its maximum value, 424 MPa (at 5mm from the weld center). Afterwards, the residual stresses decrease and become zero at 28 mm far from weld line. It can be concluded that using LTT filler leads to a reduction in the tensile residual stresses in the weld zone especially tangible decrease in residual stress maximum values. It also reduced tensile residual stress span in longitudinal residual stress distribution. However, this effect is not considerable.

Transverse welding residual stresses at the middle of samples are plotted in Figure 14. It is clear that transverse residual stresses in conventional filler welding are tensile and its maximum occurs in the weld zone. However, welding with LTT filler produces

compressive stresses in weld zone, which is due to the induced expansion in low temperatures by formation of martensite.

To explain mechanism of formation residual stress and how phase transformation affects it during simulation of welding with LTT filler, the thermal-metallurgical-mechanical behavior of a point at the center of weld line is considered. In Figure 15, the evolution of thermal stress relative to time with respect to the phase transformation, during simulation of welding using LTT filler has been illustrated. It can be seen, martensite is transformed to austenite when the heat source reaches the selected point and hence temperature rises rapidly. Austenite stays stable until the temperature drops below the M_s temperature and after that, the martensitic transformation begins. Percentage of martensite increases with decreasing temperature which indicates increasing in volume expansion. For temperatures higher than M_s , thermal stresses are tensile while volume expansion due to martensitic transformation causes a sudden decrease in stresses and changes rising trends to decreasing trend which is related to the increasing percentage of martensite in microstructure for lower temperatures.

Evolution of phase fraction and thermal stress for the same point as previous in the simulation of welding with the conventional filler has been illustrated in Figure 16. As can be seen, the initial microstructure of the conventional filler is 100% ferrite, which is transformed to austenite bypassing the heat source. As the austenite temperature decreases, it decomposes into ferrite and bainite which is not accompanied with a tangible volume changes. Therefore, the evolution of thermal stress relative to the time indicates that when using the conventional filler, the thermal contraction is the dominant factor in the formation of welding residual stress and as a result high tensile residual stresses exist in weld region.

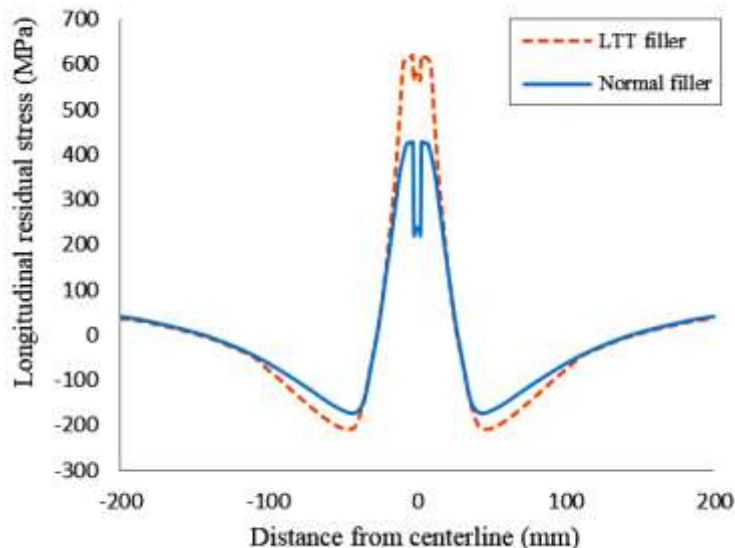


Figure 13. Distribution of longitudinal residual stresses in FEM for LTT and normal fillers.

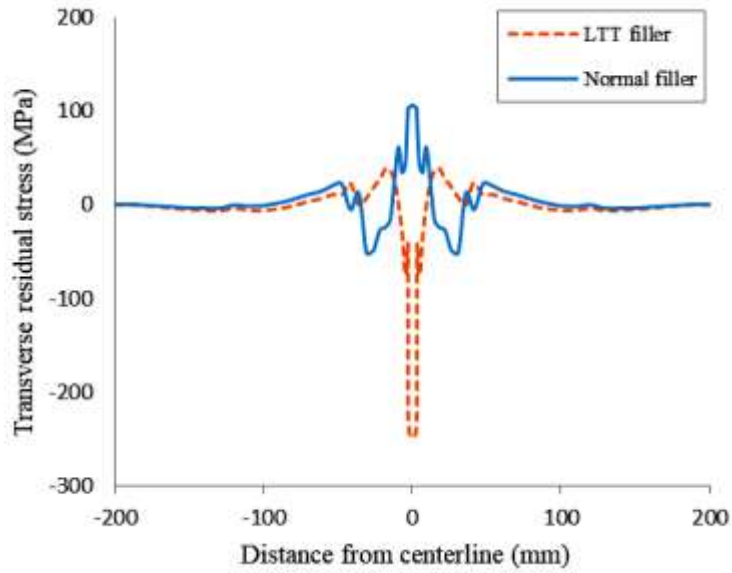


Figure 14. Distribution of transverse residual stresses in FEM for LTT and normal fillers.

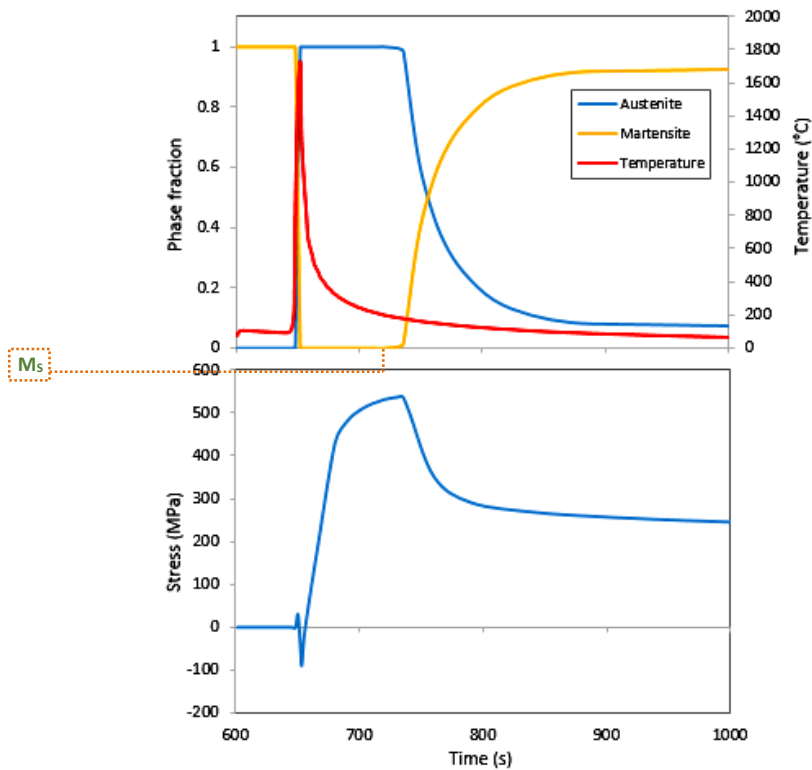


Figure 15. Evolution of phase fraction and thermal stress relative to time in welding with the LTT filler.

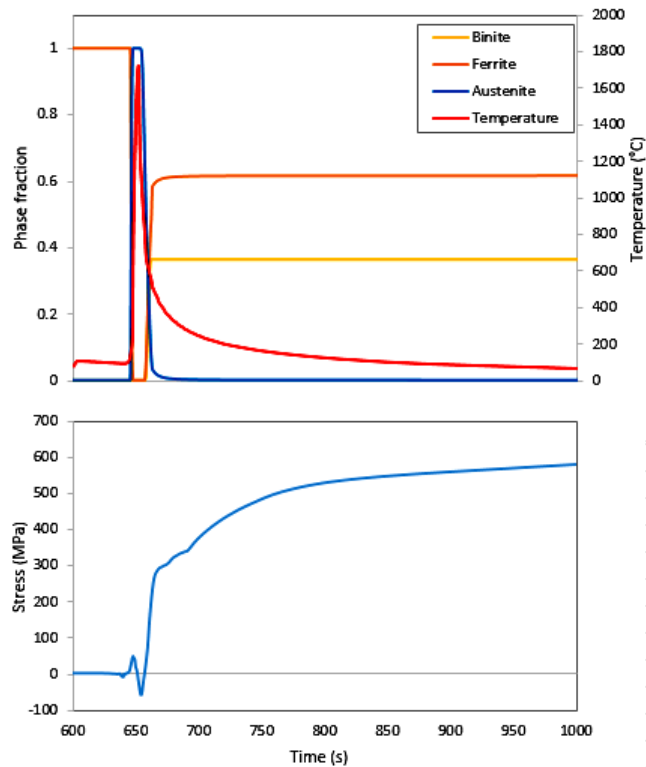


Figure 16. Evolution of phase fraction and thermal stress relative to time in welding with the conventional filler.

CONCLUSION

The aim of the present work was to investigate residual stresses changes due to application of LTT fillers. Two high-strength steel sheets were butt welded using LTT and normal fillers. ER70S-6 and ER410NiMo fillers were employed as conventional and LTT fillers, respectively. 3-D models were developed in SYSWELD to predict residual stresses. Predicted residual stresses were compared with experiments and a good agreement was observed. It can be concluded that in welding with normal filler, longitudinal and transverse residual stresses were tensile in weld line center and its adjacent areas. In welding with LTT filler, the weld metal developed a martensitic microstructure in relatively low M_s temperature during cooling. The expansion caused by low temperature transformation compromised cooling induced contraction; thus, tensile residual stresses in weld zone plummeted and even turned compressive at some points. Maximum longitudinal tensile residual stress also decreased. Longitudinal residual stress in weld line center dropped from 554 MPa to 216 MPa (decreased by 60%). On the other hand, tensile transverse residual stress in weld line center changed from 156 MPa to 289 MPa and became compressive.

REFERENCES

- [1] Yaakob K, Ishak M, Idris S. The effect of pulse welding parameters on weld geometry of boron steel using low power fibre laser. *Journal of Mechanical Engineering and Sciences* 2017;11(3):2895-905.
- [2] Ooi S, Garnham J, Ramjaun T. Low transformation temperature weld filler for tensile residual stress reduction. *Materials & Design* 2014;56:773-81.
- [3] Hussin MH, Lah NAC. Effects of temperature on the surface and subsurface of Al-Mg-Si welded joints. *Journal of Mechanical Engineering and Sciences* 2017;11(2):2743-54.
- [4] Masubuchi K. Recent MIT research on residual stresses and distortion in welded structures. 1993.
- [5] Zenitani S, Hayakawa N, Yamamoto J, Hiraoka K, Morikage Y, Kubo T, et al. Development of new low transformation temperature welding consumable to prevent cold cracking in high strength steel welds. *Science and Technology of Welding and Joining* 2007;12(6):516-22.
- [6] Kannengiesser T, Kromm A, Rethmeier M, Gibmeier J, Genzel C. Residual stresses and in situ measurement of phase transformation in low transformation temperature (LTT) welding materials. *Advances in X-ray Analysis* 2009;52:755-62.
- [7] Camilleri D, McPherson N, Gray TG. The applicability of using low transformation temperature welding wire to minimize unwanted residual stresses and distortions. *International Journal of Pressure Vessels and Piping* 2013;110:2-8.
- [8] Özdemir O, Çam G, Çimenoğlu H, Koçak M. Investigation into mechanical properties of high strength steel plates welded with low temperature transformation (LTT) electrodes. *International Journal of Surface Science and Engineering* 2012;6(1-2):157-73.
- [9] Özdemir O, Çam G, Çimenoğlu H, Koçak M. Characterization of Microstructure and Mechanical Properties of Low Temperature Transformation Welds (LTT). In: 13th International Materials Symposium (IMSP 2010), Turkey, 2010.
- [10] Barsoum Z, Gustafsson M. Fatigue of high strength steel joints welded with low temperature transformation consumables. *Engineering Failure Analysis* 2009;16(7):2186-94.
- [11] Ramjaun T, Stone H, Karlsson L, Kelleher J, Ooi S, Dalaei K, et al. Effects of dilution and baseplate strength on stress distributions in multipass welds deposited using low transformation temperature filler alloys. *Science and Technology of Welding and Joining* 2014;19(6):461-7.
- [12] Moat R, Ooi S, Shirzadi A, Dai H, Mark A, Bhadeshia H, et al. Residual stress control of multipass welds using low transformation temperature fillers. *Materials Science and Technology* 2018;34(5):519-28.
- [13] Vollert F, Dixneit J, Gibmeier J, Kromm A, Buslaps T, Kannengiesser T, editors. In situ EDXRD study of MAG-welding using LTT weld filler materials under structural restraint. *Materials Science Forum*. 2017;905:107-113.
- [14] Gach S, Olschok S, Arntz D, Reisgen U. Residual stress reduction of laser beam welds by use of low-transformation-temperature (LTT) filler materials in carbon manganese steels—In situ diagnostic: Image correlation. *Journal of Laser Applications* 2018;30(3):032416.

- [15] Deng Y JW. A Novel Method of Reducing Residual Stress: Low Transformation Temperature (LTT) Weld Filler. *Research & Development in Material Science* 2018;6(3):578-85.
- [16] Nalla R, Altenberger I, Noster U, Liu G, Scholtes B, Ritchie R. On the influence of mechanical surface treatments—deep rolling and laser shock peening—on the fatigue behavior of Ti–6Al–4V at ambient and elevated temperatures. *Materials Science and Engineering: A* 2003;355(1):216-30.
- [17] Elmer J, Olson D, Matlock D. Thermal expansion characteristics of stainless steel weld metal. *Welding Journal* 1982;61(9):293.
- [18] Martinez F, Liu S, editors. Development of compressive residual stress in structural steel weld toes by means of weld metal phase transformations. In: *Proceedings of the 7th International Conference trends in Welding Research (ASM International)*, Pine Mountain, Georgia, pp 16-20; 2005.
- [19] Payares-Asprino M, Katsumoto H, Liu S. Effect of martensite start and finish temperature on residual stress development in structural steel welds. *Welding Journal, Research Supplement* 2008;87:279s-89s.
- [20] Bhadeshia H. Martensite in steels. *Materials Science & Metallurgy*. 2002.
- [21] Çam G, Özdemir O, Koçak M, Progress in low transformation temperature (LTT) filler wires: review. In: *Proceedings of the 63rd Annual Assembly & International Conference of the International Institute of Welding*, Istanbul, Turkey, pp 759-765; 2010.
- [22] Hwang B, Lee T, Kim S. Effect of alloying elements on ductile-to-brittle transition behavior of high-interstitial-alloyed 18Cr-10Mn austenitic steels. *Procedia Engineering* 2011;10:409-414.
- [23] Alghamdi T, Liu S. Low-transformation-temperature (LTT) welding consumables for residual stress management: consumables development and testing qualification. *Welding Journal* 2014;93(7): 243s-252s.
- [24] ASTM E 837-13, Standard test method for determining residual stresses by the hole-drilling strain-gage method. West Conshohocken, PA: ASTM International, 2013.
- [25] Stamenković D, Vasović I. Finite element analysis of residual stress in butt welding two similar plates. *Scientific technical review* 2009;59(1):57-60.
- [26] Goldak JA, Akhlaghi M. *Computational welding mechanics*. 2005 ed. New York: Springer Science & Business Media; 2006.
- [27] Dutta P, Joshi Y, Franche C. Determination of gas tungsten arc welding efficiencies. *Experimental thermal and fluid science* 1994;9(1):80-9.
- [28] Mi G, Li C, Gao Z, Zhao D, Niu J. Finite element analysis of welding residual stress of aluminum plates under different butt joint parameters. *Engineering Review* 2014;34:161-166.
- [29] Francis JD. *Welding simulation of aluminum alloy joints by finite element analysis*. Virgin, USA: Virginia Polytechnic Institute and State University; 2002.
- [30] Jeyakumar M, Christopher T, Narayanan R, Rao B. Residual Stress Evaluation in Butt-welded IN718 Plates. *Canadian Journal of Basic and Applied Sciences* 2013;01:88-99.